in cross section by about 10^5 and that appears to be *consistent with experimental data over this range.* The model is a natural extension of the strong absorption model for describing single Reggeon exchanges, so if our considerations are correct, an internally consistent approach is available for discussing all nondiffractive two-body hadronic reactions. Finally, we have briefly discussed the interesting possibility that one can relate the spin dependence of couplings to the size of exotic amplitudes—if the ρ-coupling did not flip s-channel baryon helicities, exotic amplitudes would be an order of magnitude larger.

*Research supported in part by the U. S. Atomic Energy Commission.

[1]M. Ross, F. S. Henyey, and G. L. Kane, Nucl. Phys. B23, 269 (1970).

[2]While we were writing this paper we became aware of the related work by H. Harari, Phys. Rev. Lett. 26, 1079 (1971). He mainly considers the qualitative experimental evidence for large DPE contributions, coming to conclusions consistent with ours and with Ref. 4.

[3]Related models have been proposed by C. Michael, Phys. Lett. 29B, 230 (1969); and by C. Quigg, thesis, University of California, Berkeley (unpublished). They have not discussed the importance of most of the features that we find dominate the result.

[4]F. Henyey, G. L. Kane, J. Pumplin, and M. H. Ross, Phys. Rev. 182, 1579 (1969).

[5]Zeros in the Regge-pole amplitude, which we do not include, would reduce the cuts significantly (Quigg, Ref. 3).

[6]G. L. Kane, F. Henyey, D. R. Richards, M. Ross, and G. Williamson, Phys. Rev. Lett. 25, 1519 (1970); F. D. Gault, A. D. Martin, and G. L. Kane, to be published.

[7]F. Henyey, G. L. Kane, and J. J. G. Scanio, to be published.

[8]C. Michael, Ref. 3, and Nucl. Phys. B13, 644 (1969).

[9]A. Lundby *et al.*, to be published.

[10]C. W. Akerlof, "Double Charge Exchange Reactions," in Proceedings of the Meeting of the Division of Particles and Fields of The American Physical Society, Austin, Texas, 5-7 November 1970 (to be published).

[11]W. Bugg *et al.*, to be published.

[12]F. Henyey, in *Proceedings of the 1969 Regge Cut Conference, Madison, Wisconsin,* edited by P. M. Fishbane and L. M. Simmons, Jr. (University of Wisconsin, Madison, Wis., 1969).

[13]J. Rosner, private communication.

[14]P. J. O'Donovan, to be published, raises this example.

Comparison of an Inclusive Multiperipheral Model to Secondary Spectra in p-p Collisions*

Clifford Risk†
Lawrence Radiation Laboratory, University of California, Berkeley, California 94720, and Department of Physics, University of California, Davis, California 95616

and

Jerome H. Friedman
Lawrence Radiation Laboratory, University of California, Berkeley, California 94720

(Received 5 April 1971)

The quantitative predictions of an inclusive multiperipheral model are compared with the measured secondary spectra in pp collisions from 12 to 30 GeV/c.

For proton-proton collisions at high energies the dominant contributions to the total cross section come from inelastic processes. The simplest probe of these processes are inclusive experiments of the type $p+p \to x+$anything, where x is one of the several types of final-state particles (e.g., $\pi^{\pm}$, $K^{\pm}$, or p). The usual procedure is to measure the momentum spectra of x for various angles of its production. Recently, three such experiments have been performed at 12.4,[1] 19.2,[2] and 30 GeV/c.[3] In this report we show that the prominent characteristics of these spectra can be understood with a simple multiperipheral model that contains the known properties of two-body scattering processes. We compare the $\pi^{\pm}$, $K^{\pm}$, and proton spectra measured by these experiments to the predictions of an inclusive multiperipheral model that is a modified version of that first proposed by Caneschi and Pignotti (CP).[4]

Our modified CP inclusive multiperipheral model is illustrated by the diagrams of Fig. 1. Figure 1(a) represents the case of the proton remaining at the end of the multiperipheral chain; Fig. 1(b) represents the baryon-exchange case of the proton traveling down one link, emitting a

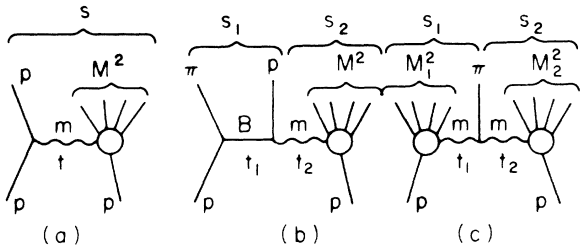

FIG. 1. Diagrams representing the processes comprising the inclusive multiperipheral model described in the text.

pion at the end of the chain; and Fig. 1(c) characterizes the pions produced at the internal links. In all three cases the remaining links in the multiperipheral chain are simulated by the inelastic scattering of an exchanged meson m with the remaining incident protons. This model primarily differs from CP in that the fast mesons and slow protons are described by a single diagram [Fig. 1(b)] instead of the three diagrams used by CP. This eliminates the the need for extrapolating the $\bar{p}p$ total cross section below threshold, and allows us to describe the fast mesons directly in terms of the backward meson-baryon elastic differential cross sections.

As derived by CP on the basis of a multi-Regge model, the matrix elements squared for the processes corresponding to the diagrams of Figs. 1(a)–1(c) can be expressed, respectively, as

$$R_1 = (s/M^2)^{2\alpha_m(t)}\beta_m^2(t)M^2\sigma_T(M^2),$$

$$R_2 = s_1^{2\alpha_B(t_1)}(s_2/M^2)^{2\alpha_m(t_2)} \times \beta_B^2(t_1)\beta_m^2(t_2)M^2\sigma_T(M^2),$$

$$R_3 = (s_1/M_1^2)^{2\alpha_m(t_1)}(s_2/M_2^2)^{2\alpha_m(t_2)} \times \beta_m^2(t_1)\beta_m^2(t_2)M_1^2\sigma_T(M_1^2)M_2^2\sigma_T(M_2^2).$$

For all three diagrams the exchanged meson trajectories are chosen to be the same and are set equal to the effective ρ-meson trajectory given by Fox.[5] The exchanged-baryon trajectories are represented by the known s and t dependence of the backward meson-baryon elastic scattering.[6-9] The exchanged-meson-baryon total cross section is taken to be slowly falling from threshold to an asymptotically constant value $-\sigma_T(M^2) = 24(1+0.3/M^2)$.

To describe the data with our model we use the following procedure. We adjust the meson-exchange residue function $\beta_m^2(t)$ to best describe the shape of the pion p_T^2 spectrum at the smallest p_L measured in the 12.4-GeV/c data of Ref. 1. We find $\beta_m^2(t)$ equal to $e^{2.1t}$ for $t > -0.3$, and $ce^{0.3t}$ for $t < -0.3$. We adjust the baryon-exchange residue function $\beta_B^2(t)$ to best describe the p_T^2 dependence of the pions with large p_L using the 19.2-GeV/c data of Ref. 2. We obtain $\beta_B^2(t)$ equal to $e^{1.5t}$ and $t > 0.2$ and $c'e^{0.2t}$ for $t < 0.02$. Here the constants c and c' are inserted simply to insure continuity. We normalize the contribution of Fig. 1(a) to reproduce the magnitude of the fast (large-p_L) protons and of Fig. 1(b) to reproduce the magnitude of the fast pions, both at 19.2 GeV/c. The contribution of Fig. 1(c) is normalized to the magnitude of the slow (small-p_L) pions at 12.4 GeV/c.[10] The complete π^+, π^-, and proton spectra are now predicted at all three energies. We now discuss the salient features of these measured spectra and their description in terms of this model.

The proton spectra (Fig. 2).—The process of Fig. 1(a) gives rise to elastic forward-produced protons and hence a sharp peaking in the proton p_T^2 spectra. The process of Fig. 1(b) gives rise to more inelastic larger-angle protons since the proton emits a pion before scattering from the

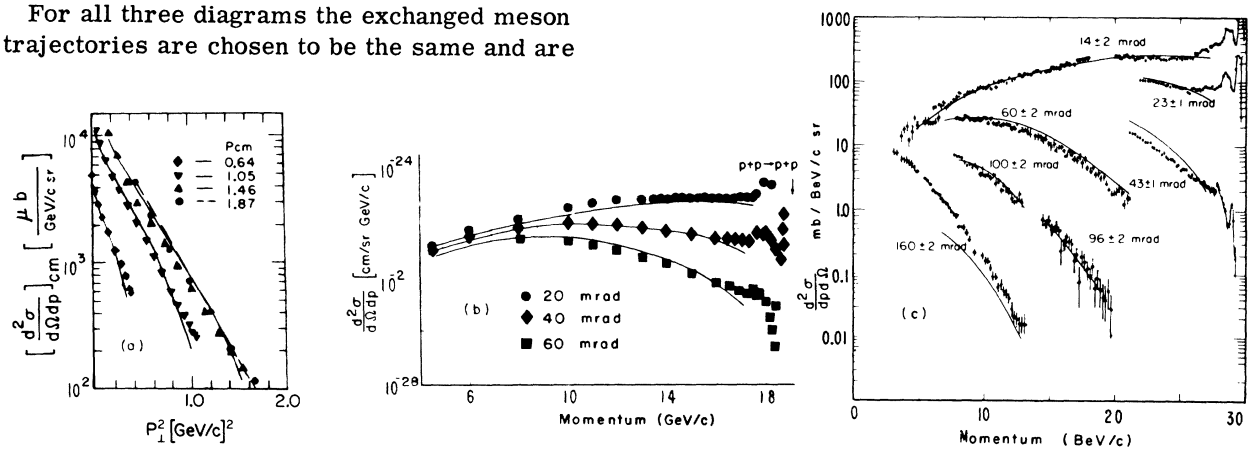

FIG. 2. Proton spectra measured at (a) 12.4 GeV/c (Ref. 1), (b) 19.2 GeV/c (Ref. 2), (c) 30 GeV/c (Ref. 3). The solid lines are the predictions of the model.

other incident proton and hence emerges on the average at a larger angle and lower momentum than the single-scattered protons of Fig. 1(a). Therefore this model predicts that the p_T^2 distribution will become more sharply peaked at large longitudinal momenta, a result confirmed by the experimental data.

The protons with large longitudinal momenta arising from the process of Fig. 1(a) account for the background to the structure observed near the kinematical limit at 19.2 and 30 GeV/c [Figs. 2(b) and 2(c)]. This structure could have been reproduced with our model by including the low-energy resonances in the meson-proton total cross section $\sigma_T(M^2)$.

Pion transverse-momentum spectra.—Figure 3(a) displays the p_T^2 spectra of the $\pi^\pm$ at 12.4 GeV/c as measured by Akerlof *et al.*[1] These distributions are both characterized by a sharp peak $[\exp(-15p_T^2)]$ for small p_T^2 that levels off to a more gentle dependence $[\exp(-3p_T^2)]$ for larger p_T^2. As for the protons, the sharp peaking of the pions comes from the forward pions produced at the end of the multiperipheral chain in the baryon-exchange process of Fig. 1(b), while the more slowly falling part of the spectrum for larger p_T^2 arises from the pions produced at intermediate links.[11,12]

Pion longitudinal-momentum spectra.—The data at 12.4 and 19.2 GeV/c (Refs. 1 and 2) show the π^- spectrum falling much more rapidly at large values of p_L than that of the π^+ [Figs. 3(a)-3(d)]. For the 19.2-GeV/c data, in the interval from $p = 10$ to 16 GeV/c the π^- rate decreases 5 times faster than the π^+ rate. In our model this arises from the difference between $\pi^- p$ and $\pi^+ p$ backward elastic scattering in the process of Fig. 1(b). The backward $\pi^- p$ elastic cross section is smaller in magnitude and falls faster from the resonance region than the corresponding $\pi^+ p$ cross section.[6] Since the very fastest pions result from large πp subenergy in Fig. 1(b), the

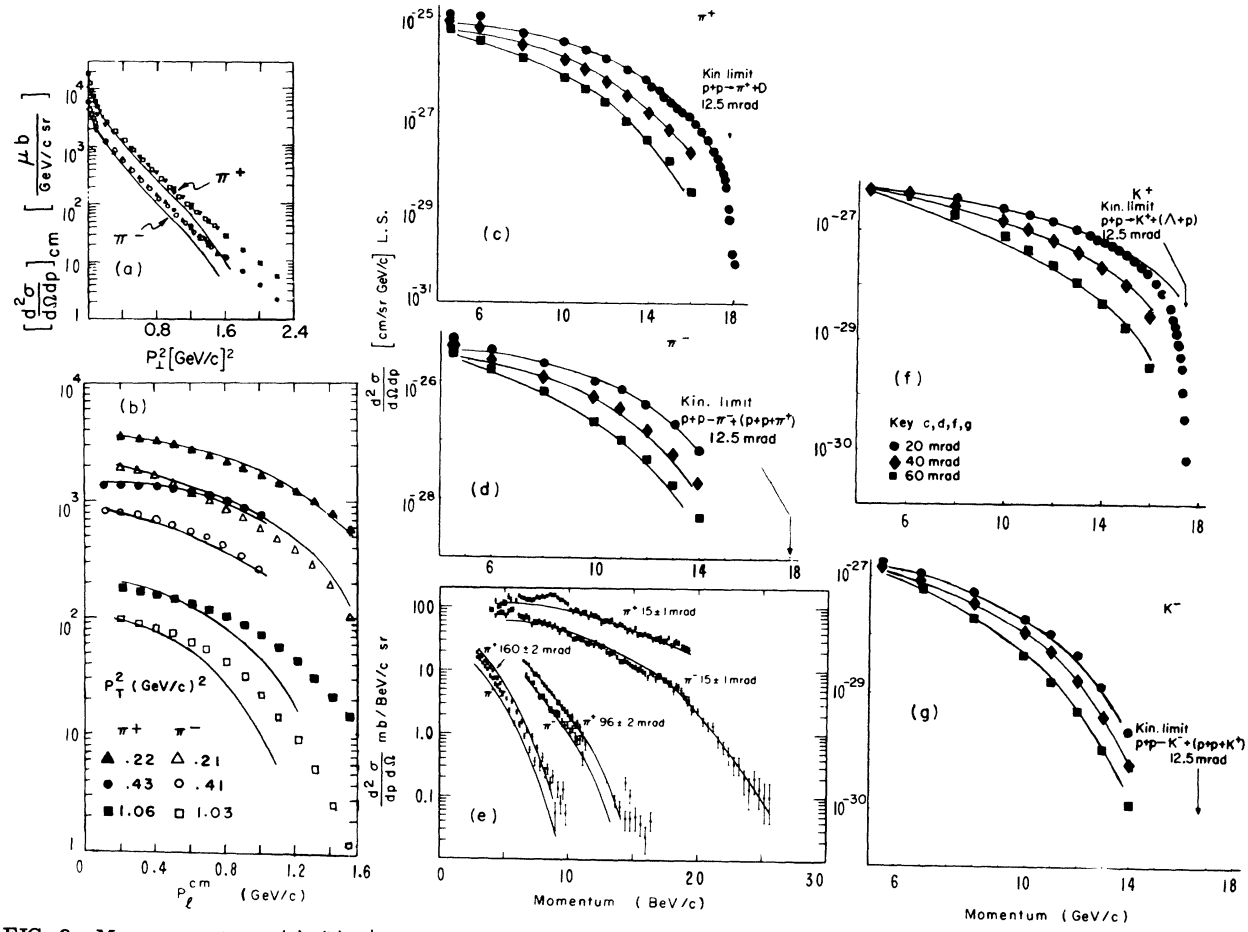

FIG. 3. Meson spectra. (a), (b) $\pi^\pm$ at 12.4 GeV/c (Ref. 1); (c), (d) $\pi^\pm$ at 19.2 GeV/c (Ref. 2); (e) $\pi^\pm$ at 30 GeV/c (Ref. 3); and (f), (g) $K^\pm$ at 19.2 GeV/c (Ref. 2). The solid lines are the predictions of the model.

relative smallness of the $\pi^- p$ as compared to the $\pi^+ p$ backward elastic cross sections at the large subenergies ($s_1 \sim 10$ GeV^2) results in the relative depletion of the π^- with large p_L.

The $K^\pm$ spectra.—The relation imposed by this model between fast meson secondaries and the cross section for meson-proton backward elastic scattering should be even more pronounced for the $K^\pm$ spectra than the $\pi^\pm$ spectra since the $K^- p$ backward elastic cross section falls with increasing energy much more rapidly than that for the backward $K^+ p$.[7] We find that the K^- spectrum of Fig. 3(g) is described entirely by Fig. 1(c), while the K^+ spectrum in Fig. 3(f) requires Fig. 1(c) for slow mesons and Fig. 1(b) for fast mesons. The lack of fast K^- relative to K^+ is apparent in the measured spectra and is adequately described by our model.

To summarize, we have compared the quantitative predictions of a fairly restrictive inclusive multiperipheral model to the meson and proton spectra resulting from pp collisions at three momenta from 12 to 30 GeV/c. There are some discrepancies between the predictions of our model and the measured spectra that could perhaps be reduced by further adjustment of some parameters, but the results taken together suggest a consistent view of features of inclusive data in terms of two-body data.

We thank V. Chung for helpful discussions during the formative stages of this work, especially concerning the p_T^2 peaking mechanism. We also express our gratitude to J. Ball, G. Kane, G. Lynch, G. Marchesini, and M. Ross for useful discussions.

*Work supported in part by the U. S. Atomic Energy Commission.

†Participating guest at Lawrence Radiation Laboratory, Berkeley, Calif. 94720.

[1]C. W. Akerlof *et al.*, Phys. Rev. D 3, 645 (1971).

[2]J. V. Allaby *et al.*, to be published.

[3]E. W. Anderson *et al.*, Phys. Rev. Lett. 19, 198 (1967).

[4]L. Caneschi and A. Pignotti, Phys. Rev. Lett. 22, 1219 (1969).

[5]G. Fox, in *High Energy Collisions—Third International Conference*, edited by C. N. Yang, J. A. Cole, M. Good, R. Hwa, and J. Lee-Franzini (Gordon and Breach, New York, 1970), p. 367.

[6]L. Anderson *et al.*, Phys. Rev. D 3, 1536 (1971).

[7]L. Price *et al.*, Lawrence Radiation Laboratory Report No. UCRL-20000 K^+N, 1969 (unpublished).

[8]E. Berger and G. Fox, Nucl. Phys. B26, 1 (1971).

[9]We parametrize the backward differential cross section as $d\sigma/du = \beta^2(u) s^{2\alpha(u)-2}$, and from the experimentally measured cross sections in the energy range $3 < s < 6$ GeV^2 (Refs. 6, 7) we determine $\alpha(0)$ to be -2.0 for $\pi^- p$, -1.3 for $\pi^+ p$, and -0.25 for $K^+ p$. The shape of $\alpha(u)$ is taken from Ref. 8.

[10]We find that the process of Fig. 1(c) accounts for 80% of the meson spectrum, while Fig. 1(b) gives rise to the remaining 20%. Figure 1(a) accounts for about 50% of the proton spectrum and Fig. 1(b) for the rest.

[11]For $p_T^2 \gtrsim 1.6$ GeV^2, where $t_1 \simeq -4$ GeV^2 and the angle of the emitted pion is greater than 60°, the simple Regge-pole representation of the two-body scattering amplitudes becomes invalid and the model undercuts the spectrum [Fig. 3(a)].

[12]We find that Fig. 1(c) also predicts a sharp p_T^2 peaking for $p_T < 0.3$ GeV/c at $p_L \sim 0$.

$\bar{K}N$ Interaction in the Region 0 to 1200 MeV/c and Hyperon Resonances*

Jae Kwan Kim
Department of Physics, Harvard University, Cambridge, Massachusetts 02139
(Received 28 March 1971)

A multichannel phase-shift analysis has been performed for the first time on the available experimental data of all the channels of $\bar{K}N$ interactions in the momentum region 0 to 1200 MeV/c. The Argand diagrams of the reaction amplitudes and the resonance parameters within the momentum region are given. The results provide stronger evidence for a number of previously suggested resonances and also indicate some new possible resonances.

The experimental data for the following reactions below the incident $\bar{K}$ momentum of 1200 MeV/c have been accumulating very rapidly during the last five years: $\bar{K}N$ interacting into $\bar{K}N$, $\Sigma\pi$, $\Lambda\pi$, $\bar{K}N\pi$, $\Sigma\pi\pi$, $\Lambda\pi\pi$, and $\Lambda\eta$ final channels. It has become possible to make a meaningful multichannel phase-shift analysis incorporating simultaneously the existing data of all the above